PNAS
www.pnas.org

Supplementary Information for
Three small vesicular pools in sequence govern synaptic response dynamics during action potential trains

Van Tran[a,1,2], Takafumi Miki[b,1,2], and Alain Marty[a]

[a]Université de Paris, SPPIN-Saints Pères Paris Institute for the Neurosciences, CNRS, F-75006 Paris, France; [b]Graduate School of Brain Science, Doshisha University, 1-3 Tatara Miyakodani, Kyotanabe-shi, Kyoto, 610-0394, Japan.

[1]These authors contributed equally.

[2]To whom correspondence may be addressed: Email: le-thuy-van.tran@parisdescartes.fr; tmiki@mail.doshisha.ac.jp

This PDF file includes:

Materials and Methods

Preparation and recording procedures

200 μm thick sagittal slices were prepared from the cerebellar vermis of Sprague-Dawley rats (P12–17). Slices were incubated at 34 °C for at least 45 min before the beginning of recordings.

Whole-cell patch-clamp recordings were obtained from molecular layer interneurons (MLIs; comprising both basket and stellate cells). The extracellular solution contained (in mM): 130 NaCl, 2.5 KCl, 26 $NaHCO_3$, 1.3 NaH_2PO_4, 10 glucose, 3 $CaCl_2$, and 1 $MgCl_2$. It was equilibrated with 95% O_2 and 5% CO_2 (pH 7.4). The internal recording solution contained (in mM): 144 K-gluconate, 6 KCl, 4.6 $MgCl_2$, 1 EGTA, 0.1 $CaCl_2$, 10 HEPES, 4 ATP-Na, 0.4 GTP-Na (pH 7.3, 300 mosm/l). All recordings were done at 32–34 °C.

To obtain a single PF-MLI connection, an MLI was first patched and held at –60 mV. NMDA and $GABA_A$ receptors were blocked by bath application of D-APV (50 μM) and gabazine (3 μM). A monopolar pipette was then filled with the internal solution and placed above the granule cell layer. Puffs of the high K^+ internal solution was applied by mouth through the pipette to identify a potential presynaptic granule cell (1). The granule cell was then stimulated electrically and extracellularly, using the same pipette. The stimulation voltage was adjusted and kept at a minimum. If the resultant EPSCs, especially those that occurred after a short stimulation train, were homogenous, then it was likely that only one presynaptic cell was activated.

To determine the recovery kinetics of various SV pools after a short AP train, a pair of AP trains, each with 8 stimulation pulses (pulse duration: 0.10–0.15 ms; frequency: 200 Hz), were applied repetitively at 10–12 s intervals. The inter-train intervals (i.e. the time difference between the last stimulation of the first train and the first stimulation of the second train) were varied from 40 to 3965 ms, and were interleaved. For each synapse, 10-40 repeats were obtained for each inter-train interval. To assess the recovery of docked and replacement sites after prolonged stimulation, a series of twin APs were applied at various intervals (from 50 ms to 10 s) after a train of 40 APs evoked at 200 Hz (Fig. 5A, Protocol 1). In a different set of experiments, the recovery kinetics of the upstream pool was measured by applying a single 8-AP test train after a 40-AP train with a time interval of 100, 300, or 800 ms (Fig. 5B, Protocol 2). In both sets of experiments, at least 10 repeats were obtained for each time interval, and the inter-repeat interval was 60 s. Error bars and shaded areas in plots indicate the standard error of the mean.

Recordings were only accepted as a simple synapse recording after analysis and if the following three criteria were satisfied (2): 1) the EPSC amplitude of the second release event in a pair was smaller than that of the first, reflecting activation of a common set of receptors belonging to one postsynaptic density; 2) all the EPSC amplitudes follow a Gaussian distribution with a coefficient of variation < 0.5; and 3) the number of release events during the conditioning 8-AP or 40-AP train was stable.

Decomposition of EPSCs

First, ~10 isolated EPSCs that occurred after the AP trains were aligned and averaged together to produce an mEPSC template for a given synapse. This template was then fitted with a triple-exponential function with five free parameters (rise time, peak

amplitude, fast decay time constant, slow decay time constant, and amplitude fraction of slow decay). Next, the mEPSC template and individual data traces were deconvolved using the five parameters. Deconvolution of the mEPSC template produced a narrow spike (called spike template), while deconvolution of the data traces resulted in sequences of spikes. Each deconvolved trace was fitted with a sum of scaled versions of the spike template, yielding the timing and amplitude of each release event. The amplitude was further corrected for receptor saturation and desensitisation, using the exponential relationship between individual amplitudes and the time interval since the preceding release events. Events that were 1.7 times larger than the average mEPSC were split into two (2). The amplitude of each of these two events was chosen to be half of that of the original event, and their timing was separated by 0.1 ms.

The synaptic parameters s_{1f}, s_{2f}, and $S_{5\text{-}8}$ were determined as follows. s_{1f} was obtained by multiplying the number of SVs released within 5 ms after the 1st AP of a train (s_1) by the proportion of fast synchronous release during this time window. Similarly, s_{2f} was the product of the number of SVs released within 5 ms after the 2nd AP (s_2) and the corresponding proportion of fast synchronous release. $S_{5\text{-}8}$ was determined as the sum of SVs released within 5 ms after the 5th-8th APs.

Simulation of AP-evoked Ca^{2+} transients

The simulation parameters are as described in ref. (3). These include the geometry of the presynaptic bouton (0.9 (x) x 0.5 (y) x 0.5 (z) μm^3), the distribution of Ca^{2+} channels (3 clusters, each with 9 channels, located at the center of the x-y plane at z of 0 µm), their single-channel current (0.2 pA, following a Gaussian distribution with a half-width of 0.34 ms), and characteristics of the endogenous fixed buffer (2 mM; K_d = 50 µM), of free ATP (200 µM; K_d = 200 µM), of calretinin (100 µM; K_d = 28 µM for the initial T state and 68 nM for the R state, i.e. after Ca^{2+} has bound to one of the two cooperative binding sites), and of free basal Ca^{2+} (50 nM). The grid size was set to 90, 50, and 50 points, corresponding to a distance of 10 nm between successive points. Ca^{2+} extrusion was included on all surfaces with a rate of 0.9 ms^{-1} (4). The “local” Ca^{2+} concentration that drives fusion of docked SVs was obtained at a distance of 40 nm from the edge of Ca^{2+} channel clusters. The “global” Ca^{2+} concentration that shapes vesicle recruitment rates was obtained along the x-y plane at z of 0.25 µm.

Simulation of SV release

The number of docking sites were set to 4 and 5 for Figure 2 and Figure 6, respectively. The initial values of δ and ρ were 0.3 and 0.9, respectively. We calculated a release probability (P_r) at a docking site using the allosteric model of Lou et al. (ref. (5)) with the following parameter values: k_{on} = 5 x 10^8 $M^{-1}s^{-1}$, k_{off} = 5000 s^{-1}, b = 0.75, γ = 2800 s^{-1}, and f = 31.3. For the refractory period at a docking site (further described below), slow P_r was calculated with k_{on} = 5 x 10^7 $M^{-1}s^{-1}$, k_{off} = 2000 s^{-1}, b = 0.5, γ = 2000 s^{-1}, and f = 31.3. The slow P_r recovered linearly to the normal value with a recovery time of 40 or 150 ms (see below). The recruitment from a replacement site to the associated docking site was defined using a Michaelis-Menten reaction with V_{max} = 800 s^{-1} and K_d = 2 µM. The simulated local and global [Ca^{2+}] were used for P_r and recruitment rates (R_f, S_f, and S_{IP}), respectively.

For Figure 2, the pool upstream of replacement sites was supposed to be infinite in the control condition. Recruitment from the upstream pool (S_f) to each replacement site was

then defined using a Michaelis-Menten reaction having parameters S_{max} = 60 s^{-1} and K_d = 2 μM. In test cases, simulation of a depleted upstream pool was obtained by reducing the value of S_{max}. The normal P_r parameters were used for the first 2 release events in an AZ. Subsequent release events occurred with the normal P_r if they happened at a docking site that had not released yet, and with a smaller P_r in the other case. In the latter case, the smaller P_r was calculated using the slow P_r, normal P_r and the time interval since the previous release event at the same docking site, since P_r recovered linearly from the slow P_r to normal P_r during a recovery time of 40 ms (3). To see the direct effects of changing δ, ρ and S_{max} on s_{1f}, s_{2f} and $S_{5\text{-}8}$, we applied the change in the parameter values at the beginning of the 1st response (at 10.05 ms).

For Figure 6, we introduced an intermediate pool (IP) having 8 SVs above the replacement sites. Each SV site in the IP was replenished from an infinite pool with a time constant of 0.35 s. In parallel, each SV site in the IP was replenished from an infinite pool with a probability defined using a Hill equation having V_{max} = 30 s^{-1}, K_d = 5 μM, and n = 5. The recruitment from the IP to each replacement site was defined using a Michaelis-Menten reaction with S_{max} = 90 s^{-1} and K_d = 2 μM, and it changed proportionally with the remaining number of SVs in the IP. Thus, the rate of vesicular transfer for one free replacement site was S_f n/n_o, where n was the current number of SVs in the IP, and n_o the initial number. In the model, we introduced an additional parameter called membrane capacity, the value of which increased by 1 whenever an SV was released at the AZ. The membrane capacity returned to 0 with a time constant of 0.1 s. If the membrane capacity is >5, subsequent release events occurred with the normal P_r parameters if they happened in a docking site that had not released yet, and with a smaller P_r in the other case. Again, in the latter case, the smaller P_r was linearly extrapolated between the slow and normal P_r values with a recovery period of 150 ms.

We performed the calculation 3000-5000 times in a given condition using Igor Pro, and used the averaged value as results.

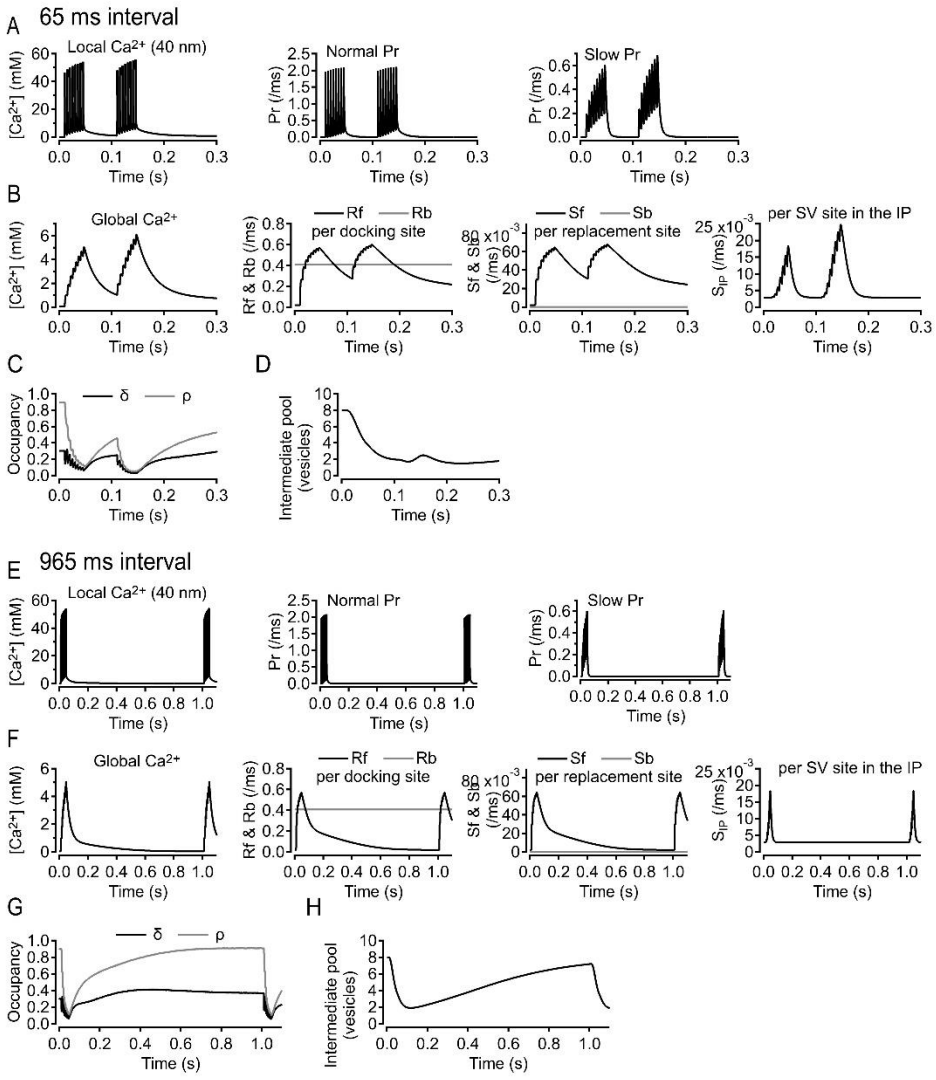

Supplementary Figure 1: Values of parameters for the simulation of two 8-AP trains.

A: Left: Profile of local $[Ca^{2+}]$ at 40 nm distance from Ca^{2+} channel clusters for two 8-AP trains with an interval of 65 ms. Middle: Normal Pr was calculated from the local $[Ca^{2+}]$ using the standard allosteric model (k_{on} = 5 x 10^8 $M^{-1}s^{-1}$, k_{off} = 5000 s^{-1}, b = 0.75, γ = 2800 s^{-1}, and f = 31.3). Right: Slow Pr was calculated from the local $[Ca^{2+}]$ using modified parameters (k_{on} = 5 x 10^7 $M^{-1}s^{-1}$, k_{off} = 2000 s^{-1}, b = 0.5, γ = 2000 s^{-1}, and f = 31.3). **B:** Left: Profile of global $[Ca^{2+}]$ for the same inter-train interval. Second left: R_f was calculated from the global $[Ca^{2+}]$ using a Michaelis-Menten reaction having a maximum speed of 800 s^{-1} and a K_d of 2 µM. The value of R_b was set such that the occupancies of docking site (δ = 0.3) and replacement site (ρ = 0.9) stayed constant at the resting state assuming $[Ca^{2+}]_{rest}$ = 50 nM. Third left: S_f was calculated from the global $[Ca^{2+}]$ using a Michaelis-Menten reaction having a maximum speed of 90 s^{-1} and a K_d of 2 µM. The value of Sb was set such that ρ stayed constant at 0.9 at rest. Right: S_{IP} had two components: the Ca^{2+}-independent component had a time constant of 0.35 s (corresponding to a rate of 2.85 x 10^{-3} ms^{-1}); the Ca^{2+}-dependent component was calculated from the global $[Ca^{2+}]$ using a Hill equation with a K_d of 5 µM, a Hill coefficient n of 5, and a maximum speed of 30 s^{-1}. **C:** The occupancies of docking site (DS) and replacement site (RS) for the same inter-train interval. **D:** The number of vesicles in the intermediate pool for the same inter-train interval (here, starting with a resting size of 8). **E-H:** Similar to A-D but with an inter-train interval of 965 ms.

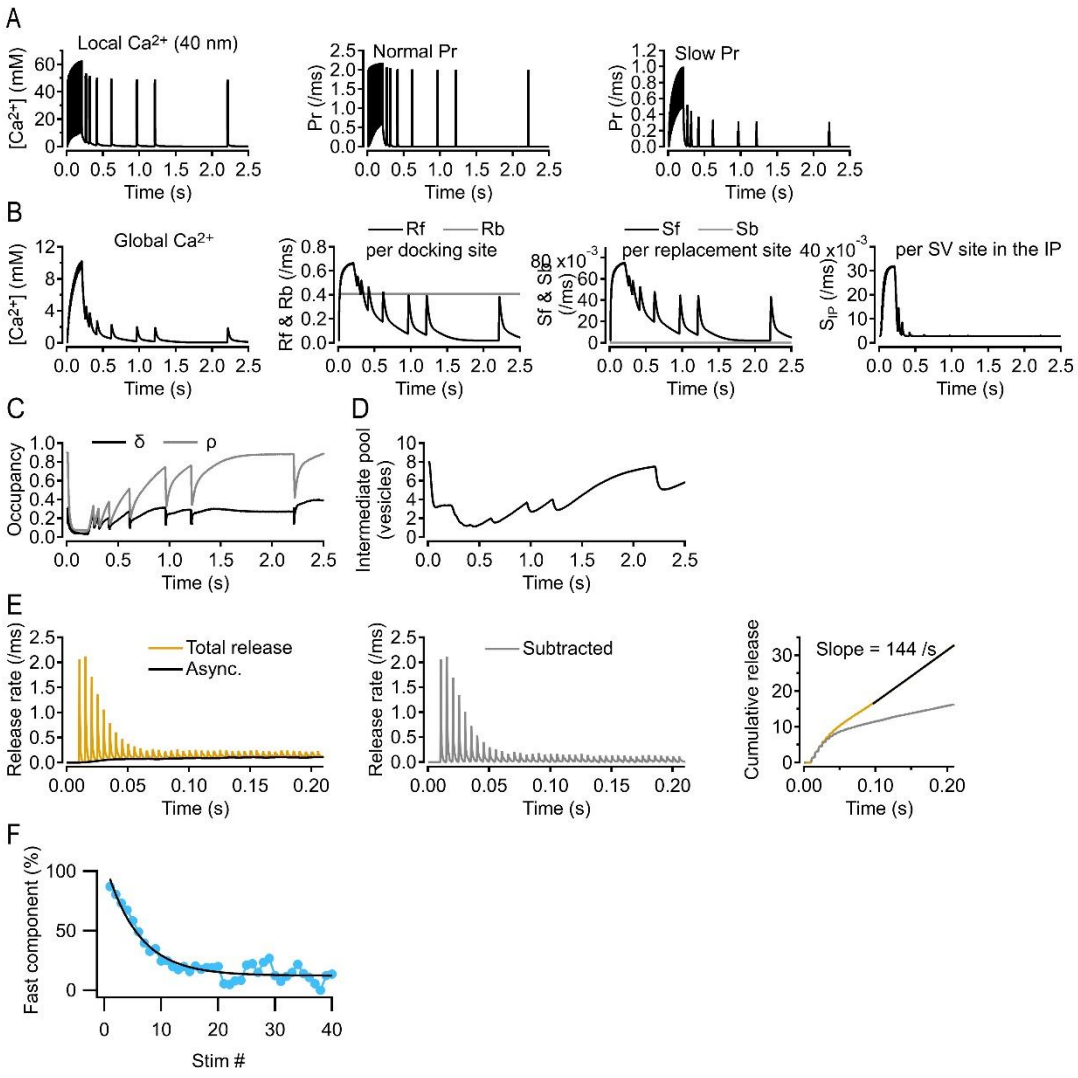

Supplementary Figure 2: Values of parameters for the simulation of 40-AP train

A: Left: Profile of local [Ca^{2+}] at 40 nm distance from Ca^{2+} channel clusters for a 40-AP train followed by twin test stimuli at various intervals. Middle and right: Normal Pr and slow Pr were calculated from the local [Ca^{2+}] as described in Supplementary Figure 1. **B:** Left: Profile of global [Ca^{2+}] for the same stimulation protocol. Second left, third left, and right: R_f, R_b, S_f, S_b, and S_{IP} were calculated from the global [Ca^{2+}] as described in Supplementary Figure 1. **C:** The occupancies of docking site (DS) and replacement site (RS) during the same stimulation protocol. **D:** The number of vesicles in the intermediate pool during the same stimulation protocol (here, starting with a resting size of 8). **E:** Left: Simulated overall release rate (total release) and the associated asynchronous component (Async.) during the 40-AP train. Middle: The corresponding synchronous component. Right: Cumulative release curves for synchronous (grey) and total release (yellow). A linear fit to the late part of the total release curve yields a limiting slope of 143 SV/s. **F:** The relative amplitude of synchronous release attributed to fast release plotted as a function of AP number obtained from the simulation. Plot was fitted with an exponential function with a time constant of 5.8 stimuli and a steady-state value of 12%.

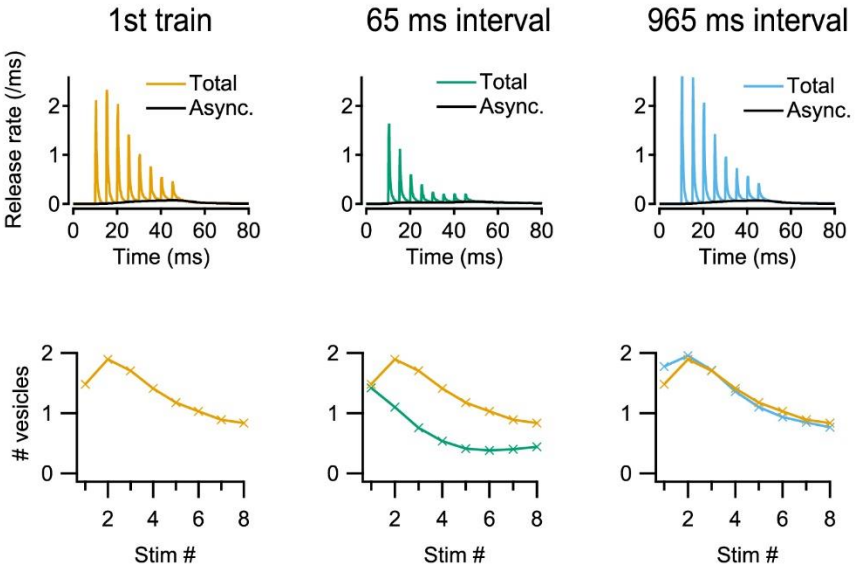

Supplementary Figure 3: Simulated SV release during two 8-AP trains

Top row: The overall release rates (total) and the associated asynchronous component (Async.) for the 1st train (left), the 2nd train after 65 ms interval (middle), and the 2nd train after 965 ms interval (right). These simulations assume a resting IP size of 8. Bottom row: The corresponding number of released SVs after individual APs. Data for the 1st train are shown together with those of the 2nd train for comparison.

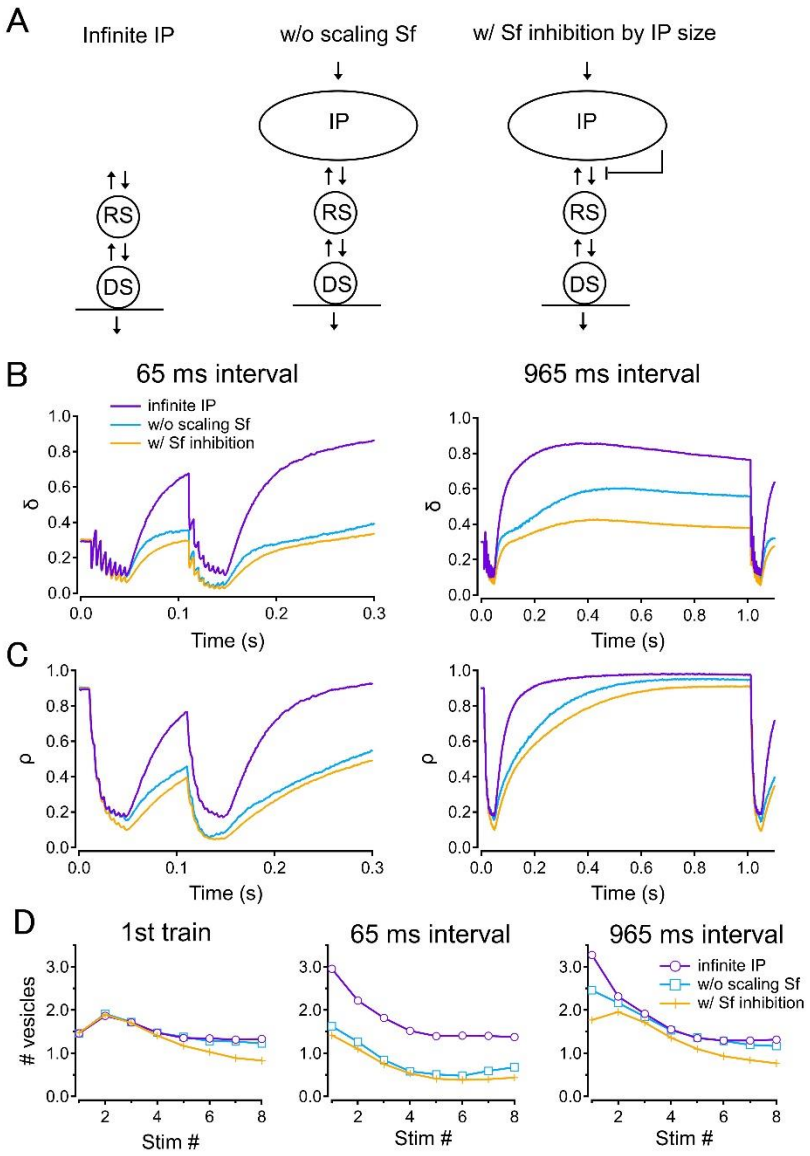

Supplementary Figure 4: Simulation of various modes of IP refilling

A: Three modes of IP refilling are simulated. In the left panel, the IP size is assumed infinite. In the center panel, the IP size is finite, but the entry rate of SVs travelling from the IP into replacement sites is fixed. In the right panel, the IP size is finite, and the entry rate of SVs travelling from the IP into replacement sites is scaled according to the number of SVs present in the IP.
B: Predictions of the occupancy of docking sites for the three variants, when stimulating with paired 8-AP trains at 65 ms interval (left) and at 965 ms interval (right).
C: Predictions of the occupancy of replacement sites for the three variants, when stimulating with paired 8-AP trains at 65 ms interval (left) and at 965 ms interval (right).
D: Predictions of the numbers of released SVs as a function of AP number, for the first AP train (left), after a 65 ms interval (center), and after a 965 ms interval (right).

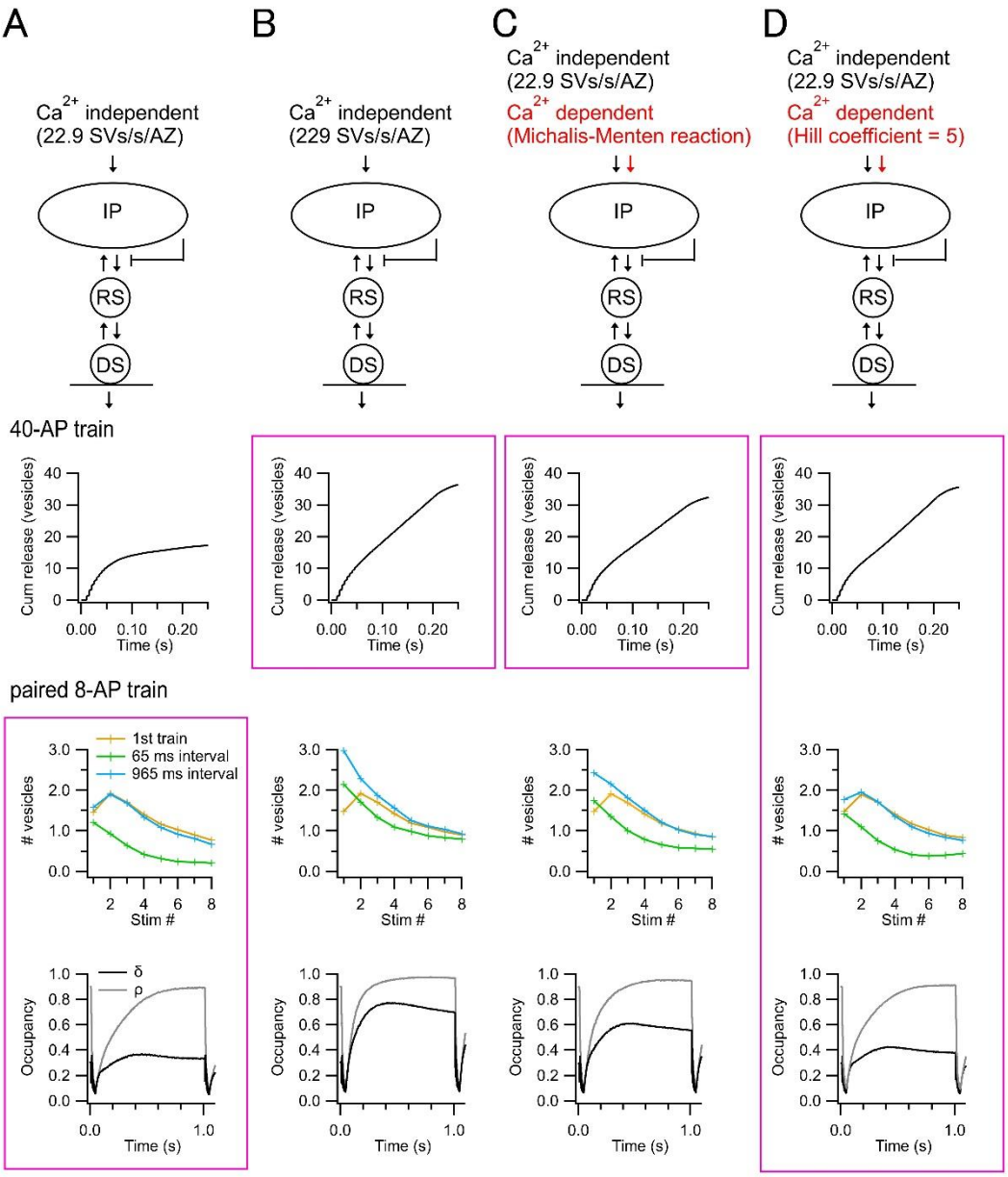

Supplementary Figure 5: Effects of dependence of S_{IP} on Ca_i and on time

A: In this model variant, S_{IP} is calcium independent, and has the value of ~23 s^{-1}. The model then predicts correctly the results for two 8-AP trains (red frame), but not for 40 APs.
B: In this model variant, S_{IP} is calcium independent, and has the value of ~230 s^{-1}. The model then predicts correctly the results for 40 APs (red frame), but not for two 8-AP trains.
C: Here S_{IP} comprises a calcium-independent part (with a value of ~23 s^{-1}), plus a part that depends on calcium with a Michaelis-Menten kinetics (K_d = 5 µM, maximum of 240 s^{-1}). Results are similar to those obtained in B.
D: As in C, except that now, the dependence of the calcium-dependent part of S_{IP} is cooperative, with a Hill coefficient of 5. Only this model correctly predicts all aspects of the data (red frame).

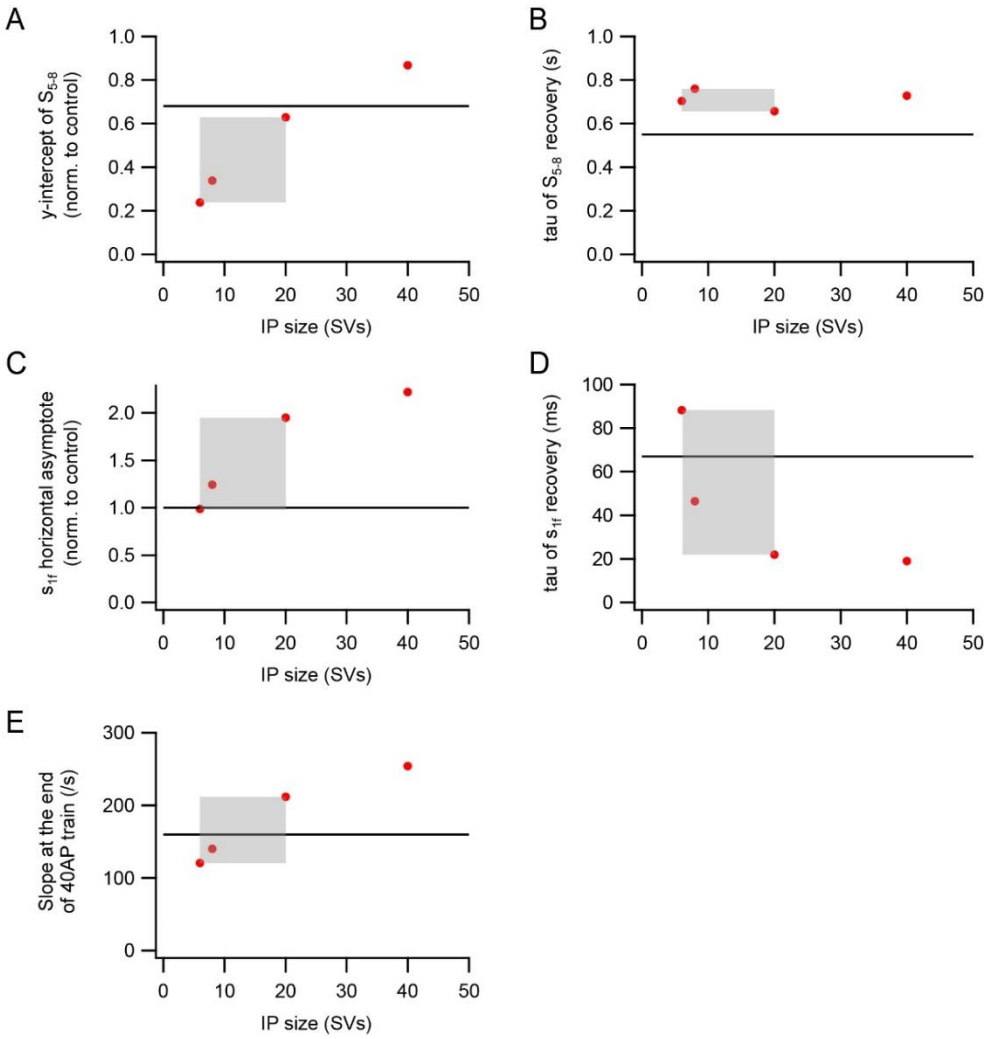

Supplementary Figure 6: Simulation results as a function of IP size

A: The y-intercept obtained from the plot of S_{5-8} vs. inter-train interval for simulations of two 8-AP trains. Black line represents the corresponding experimental value from Fig. 3Q. **B:** The time constant of S_{5-8} recovery after the first 8-AP train. Black line represents the corresponding experimental value from Fig. 3Q. **C:** The horizontal asymptote obtained from the plot of s_{1f} vs. inter-train interval for simulations of two 8-AP trains. Black line represents the corresponding experimental value from Fig. 3P. **D:** The time constant of s_{1f} recovery after the first 8-AP train. Black line represents the fast recovery time constant of s_{1f} obtained from experimental results (Fig. 3Q). **E:** The limiting slope obtained from the cumulative total release curve during the 40-AP train. Black line represents the corresponding experimental value from Fig. 4D. In A-E, grey area indicates the acceptable range of IP size.

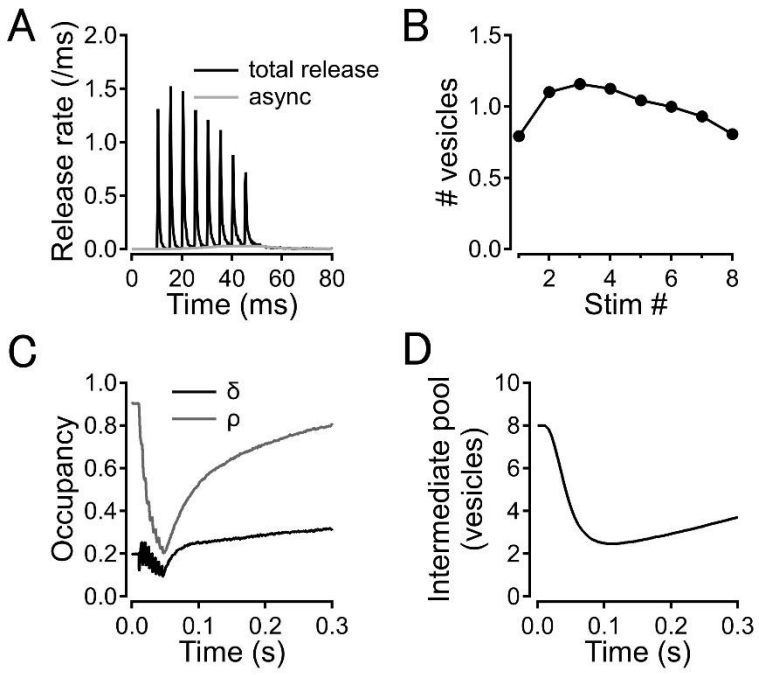

Supplementary Figure 7: Simulation of an 8-AP train in 1.5 mM Ca_o

A: Prediction of the release rates during an 8-AP train in 1.5 mM external Ca^{2+}.

B: Prediction of the number of released SVs as a function of AP number.

C: Prediction of the filling states of docking sites and of replacement sites.

D: Prediction of the filling state of the IP.

SI references

1. T. Miki, *et al.*, Numbers of presynaptic Ca2+ channel clusters match those of functionally defined vesicular docking sites in single central synapses. *Proc National Acad Sci* 114, E5246–E5255 (2017).

2. G. Malagon, T. Miki, I. Llano, E. Neher, A. Marty, Counting vesicular release events reveals binomial release statistics at single glutamatergic synapses. *J Neurosci* 36, 4010–4025 (2016).

3. T. Miki, Y. Nakamura, G. Malagon, E. Neher, A. Marty, Two-component latency distributions indicate two-step vesicular release at simple glutamatergic synapses. *Nat Commun* 9, 3943 (2018).

4. F. Helmchen, J. G. Borst, B. Sakmann, Calcium dynamics associated with a single action potential in a CNS presynaptic terminal. *Biophys J* 72, 1458–1471 (1997).

5. X. Lou, V. Scheuss, R. Schneggenburger, Allosteric modulation of the presynaptic Ca2+ sensor for vesicle fusion. *Nature* 435, 497–501 (2005).